Two-dimensional ternary locally resonant phononic crystals with a comblike coating

Yan-Feng Wang[1], Yue-Sheng Wang[1,*], and Litian Wang[2]

[1] Institute of Engineering Mechanics, Beijing Jiaotong University, Beijing, 100044, China

[2] Department of Mechanical Engineering, Østfold University College, Halden, 1757, Norway

Abstract

Two-dimensional ternary locally resonant phononic crystals used to consist of cylindrical scatterers with uniform coatings in their exterior. An alternative coating scheme with a comblike profile is proposed and investigated in this letter. The band structures are calculated by using the finite element method. It is found that a complete bandgap at a significantly low frequency can be induced. The mechanism for such a change is suggested by using an equivalent spring-mass model based on analyzing the eigen modes at the bandgap edges. Consistent results are obtained from the numerical results and the analysis of the spring-mass model.

* Corresponding author: yswang@bjtu.edu.cn (Y. S. Wang)

1. Introduction

A growing interest has been focused on the periodic, elastic structures, called phononic crystals (PCs) [1]. The PCs, composed of two or more different kind of materials with different mechanical properties and mass densities, may exhibit bandgaps, within which the propagation of elastic or acoustic waves is prohibited. Two mechanisms may give rise to bandgaps, one is the Bragg scattering, and the other is the local resonance [2]. The latter can induce a complete bandgap at a frequency which is lower by two order of the magnitude than the former one. So the locally resonant PCs may have potential applications in the control of noise or vibration at low frequencies [3].

Up to now, various kinds of locally resonant PCs have been designed [2-17]; and some equivalent analytical models are developed to evaluate the resonant frequencies [6], or the lowest bandgap [18]. Wang *et al.* [18] examined the bandgap edge modes of the ternary locally resonant PCs. At the lower edge of the bandgap, the core vibrates as a rigid sphere and the coating acts as springs. While at the upper edge of the bandgap, the core and the matrix vibrate in a reverse phase. Based on the edge modes, they developed an equivalent spring-mass model to predict the bandgap edges. In their model, only the tensile spring was considered. The tensile spring constant was calculated from the tensile elastic constant of the coating which was approximated as a plane layer between the cylinder and the matrix. Their results showed that a bandgap at a much lower frequency might be obtained by decreasing the modulus of the coating with the decrease of the bandgap width. However, it is not easy to find a material with very small modulus. Another choice is to decrease the area or volume of the coating by introducing holes. In this letter, we propose a two-dimensional comblike coating by breaking a uniform coating into N discrete pieces, see Fig.1. The sectorial pieces with the central angle of $2\Delta(=\pi/N)$ are equispaced in azimuth and oriented in the radial direction. Each piece can be regarded as a spring in vibration. It will be shown that the introduction of the free surfaces of the sectorial pieces will reduce the effective modulus of the springs, resulting in a lower resonant frequency.

2. Numerical Results

The band structures and the edge modes at the bandgap edge modes of the proposed locally resonant PC with a comblike coating are calculated by using the finite element software COMSOL. The detailed process can be found in Ref. [19]. The proposed ternary locally resonant PC is composed of cylindrical metal cores coated by rubber and embedded in the polymer matrix in a square lattice. The material parameters are listed in Table I. The inner and outer radii of the coating are r_1 and r_2, respectively. And the lattice constant is a. The band structures for the PC with a coating of 16 pieces are shown in Fig. 2(a). For comparison, the results for the PC with a uniform coating are also presented, see Fig. 2(b). Here the reduced frequency $\Omega = \omega a/(2\pi c_t)$ (with c_t being the transverse wave velocity of the matrix) is used. It is noted that a complete bandgap between the 3rd and 4th bands appears in the frequency range of $0.0282 < \Omega < 0.0572$ for the comblike coating or $0.0714 < \Omega < 0.130$ for the uniform coating, respectively. By introducing the comblike coating, the bandgap is obviously lowered as expected. The associated edge modes of displacements are shown in Fig. 3. At the lower edge of the bandgap [Figs.3(a) and 3(c)], the steel core vibrates with the coating acting as springs, while the matrix is still. At the upper edge of the bandgap [Figs.3(b) and 3(d)], the steel core and the matrix vibrate in a reverse phase. For the comblike coating, each piece plays different roles in vibration: some as tensile springs, some as shear springs, and the rest as a combination of both tensile and shear springs. The shear deformation of the comblike coating reduces the effective stiffness, and thus results in a lower bandgap.

The variation of the bandgap edges with the number of the pieces (N) is shown in Fig.4. The results for the PC with a uniform coating (N=0) are also marked in the figure. With the increase of N, the lower edge of the bandgap first decreases quickly and then tends to a fixed value ($\Omega = 0.0258$); and the upper edge of the bandgap first decreases sharply, then increases, and finally decreases in the same manner as the lower edge of the bandgap. The bandgap nearly disappears when N=2, then enlarges again at N=3 and finally nearly unchanged ($0.0258 < \Omega < 0.0523$) with N increasing. To understand the narrowing or disappearing of the bandgap at N=2, we illustrate the eigen modes of displacements for PC with the coating of two pieces in Fig.5. It is noted that the lower edge mode is similar to that of the uniform coating. While at the

upper edge of the bandgap, the steel core and the matrix vibrate in a reverse phase along the direction without the coating pieces. So in this case, different from that of the lower edge, the coating acts as shear springs with small effective stiffness, which reduces the eigen frequency of the upper edge of the bandgap significantly, narrowing or even closing the bandgap. For comparison, we calculate the band structure of the PC with a uniform coating, of which the elastic modulus is a half of rubber (because the total area of the comblike coating is a half of that of the uniform coating). The bandgap edges are shown by the two dotted lines in Fig.4. When $N\geq 3$, both lower and upper edge of the bandgaps for the comblike coating are lower than these two dotted lines, respectively. So the descent of the bandgap edges by introducing the comblike coating is not only because of the decrease of the area of the coating, but also a consequence of the shear deformation of the comblike coating. Similar trend of the changes of the bandgap edges with N is shown in the case with larger steel cores ($r_1/a=0.33$) , see Fig. 4(b). The most striking modification occurs when $N=2$, where a small complete bandgap exists. A thinner coating exhibits a larger effective stiffness and thus results in opening of this small bandgap. When $N\geq 3$, the complete bandgap tends to appear in the fixed frequency range of $0.0346 < \Omega < 0.0846$.

3. Equivalent spring-mass models

In order to understand the mechanism of the bandgap generation and estimate the bandgap edges, an equivalent mass-spring model with both tensile and shear deformation will be proposed based on the eigen modes at the bandgap edges. We first consider the PC with a uniform coating. Following the basic idea of Ref. [18], the effective masses for the lower and upper edge modes are, respectively, represented by

$$m_1 = m_{core} + \alpha m_{coating} \big/ (1+\alpha), \tag{1}$$

and

$$m_2 = m_{matrix} + m_{coating} \big/ (1+\alpha), \tag{2}$$

where $\alpha = m_2 / m_1 = (m_{matrix} + m_{coating}) \big/ (m_{core} + m_{coating})$. These equations are indeed the modification of Eq.(10) in Ref.[18].

The coating is considered as a sum of many slenders (with the central angle $\mathrm{d}\theta$)

along the radial direction, see Fig. 1(b), where θ is the angle between each slender bar and the direction of the wave propagation. Each slender bar is regarded as a tiny spring with both tensile and shear deformation. The effective tensile stiffness of a slender bar is

$$\mathrm{d}K_t = C_{11}\frac{r_1\mathrm{d}\theta}{r_2 - r_1}\cos^2\theta, \tag{3}$$

and the effective shear stiffness is

$$\mathrm{d}K_s = C_{44}\frac{r_1\mathrm{d}\theta}{r_2 - r_1}\sin^2\theta, \tag{4}$$

where $C_{11} = E(1-\nu)/((1+\nu)(1-2\nu))$ and $C_{44} = E/(2(1+\nu))$ are the elastic constants for the isotropic elastic coating with E and ν being the Young's modulus and Poisson's ratio of the coating. Then the total effective stiffness of the entire coating may be obtained by considering contributions of all these tiny springs. The result is

$$\bar{K} = \int_0^{2\pi}(\mathrm{d}K_t + \mathrm{d}K_s) = \frac{\pi r_1(C_{11} + C_{44})}{r_2 - r_1}. \tag{5}$$

Thus, the eigen frequencies can be obtained by

$$\omega_1 = \sqrt{\bar{K}/m_1}, \tag{6}$$

for the lower edge of the bandgap, and

$$\omega_2 = \sqrt{\bar{K}/m_1 + \bar{K}/m_2}, \tag{7}$$

for the upper edge of the bandgap.

The above proposed model is different from the one developed in Ref. [18]. The latter one excludes the shear deformation of the coating. However, comparison of the numerical results from FEM and predicted results by these two models, which are listed in Table II with the numbers in the brackets being the relative errors, shows that both models can give satisfied predicted results for both lower and upper edges of the bandgap with small relative errors.

The above proposed model can also be used to evaluate the lowest bandgap for the PC with a comblike coating. The predicted results are shown in Fig.4, where the thin-dashed and thin-solid lines represent the lower and upper edges of the bandgap,

respectively. They are higher than the numerical results for the comblike coating. This is because of the overestimation of the tensile spring constant of the comblike coating. It is known that the normal stress is zero on any free surface. Therefore, a thin 'surface layer' near the free surface is in the plane-stress state in each piece; while the central part is close to the plane-strain state. That is to say, for a uniform strain field, the stress in each piece is inhomogenous along the θ-direction. Therefore, this should be a two-dimensional problem. However for simplicity, we will replace it by a one-dimensional problem. In this sense, an improved one-dimensional model will be developed to evaluate the total effective stiffness of the coating.

The effective shear stiffness, immune to the free surface, is still given by Eq. (4). We will develop an improved model to calculate the effective tensile spring stiffness. For simplicity, we model each sectorial piece [Fig.6(a)] as a strip infinitely long in *z*-direction ($\varepsilon_z \equiv 0$) with the $l \times 2h$ rectangular cross-section, see Fig.6, where $l = r_2 - r_1$ and $2h = 2r_1\Delta$. Thus, the deformation of the sectorial piece along the center line can be simplified as one-dimensional tension or compression of the rectangular strip along *x*-axis. In order to describe the inhomegnous distribution of the stress, $\sigma_x(y)$, under a uniform strain in *x*-direction, ε_x, we assume that the Young's modulus is various as a function of *y*, which is denoted by $E_x(y)$ and sketched in Fig. 6(b). As mentioned before, the free surfaces ($y=\pm h$) are in the plane-stress state, i.e. $\sigma_y = \tau_{yx} = \tau_{yz} = 0$, which also implies that $\tau_{xy} = \tau_{zy} = 0$. The deformation along the *z*-direction is obviously uniform, therefore we have $\tau_{xz} = \tau_{zx} = 0$. Thus the stress-strain relation near the free surface is

$$\sigma_x = E'\varepsilon_x, \qquad (\text{at } y=\pm h) \tag{8}$$

where $E' = E_x(\pm h) = E/(1-\nu^2)$. The central part far from the free surface is close to the plane-strain state. Therefore $E_x(0)$ should be between E' and C_{11}. If the strip is very thin ($2h/l \to 0$), the whole strip is in the plane-stress state, and thus $E_x(y) \equiv E'$.

If the strip is very thick ($2h/l \to \infty$), the whole strip is in the plane-strain state, and the stress-strain relation is

$$\sigma_x = C_{11}\varepsilon_x , \tag{9}$$

i.e. $E_x(y) \equiv C_{11}$. These facts imply that $E_x(y)$ should satisfy the following constraint conditions:

$$\begin{cases} E_x(\pm h) = E' , \\ E_x(y) = E' \ \text{ when } \ 2h/l \to 0 , \\ E_x(y) = C_{11} \ \text{ when } \ 2h/l \to \infty . \end{cases} \tag{10}$$

Based on the above analysis, we write $E_x(y)$ as

$$E_x(y) = E' + (C_{11} - E')\frac{e^{2n(h-|y|)} - 1}{e^{2nh} - 1}(1 - e^{-h/l}) , \tag{11}$$

where *n* is to be determined by the numerical tests. Applying Eq.(11) to the sectorial piece in Fig.6(a), we have

$$E_r(\theta) = E' + (C_{11} - E')\frac{e^{2nr_1(\Delta-|\theta-\theta_i|)} - 1}{e^{2nr_1\Delta} - 1}(1 - e^{-nr_1\Delta/l}) \tag{12}$$

in the cylindrical coordinate, where $\theta_i = 2\pi(i-1)/N$ with $i = 1,...N$ indicating the angle formed by the center line of the *i*th piece and the vibration direction of the core, see Fig. 6(a).

To verify the rationality of the proposed model, we calculate the strain energy of two configurations. One is a sectorial piece [Fig.6(a)] subjected to an elongation along the center line. The strain energy is calculated by FEM. The other is the corresponding rectangular strip under the same elongation along *x*-axis. The strain energy is calculated with Eq.(11). The results for sectorial pieces with different central angles and those for their corresponding rectangular strips are illustrated in Fig.7. A good agreement is found between these two configurations. It is also shown that the results for the rectangular strip calculated with Eq.(11) by taking *n*=1 and 100 are almost the same. This implies that the results are almost independent of *n*. So we will take *n*=1 in the following calculation. Finally, the associated effective tensile stiffness of each tiny

spring is computed by

$$\mathrm{d}K_t' = E_r(\theta)\frac{r_1 \mathrm{d}\theta}{r_2 - r_1}\cos^2\theta\,. \tag{13}$$

Then the total effective stiffness in Eq. (5) is modified as

$$\bar{K} = \sum_{i=1}^{N}\int_{\theta_i-\Delta}^{\theta_i+\Delta}(\mathrm{d}K_t' + \mathrm{d}K_s)\,. \tag{14}$$

Evaluating the above integral, we get

$$\bar{K} = \frac{r_1}{(r_2 - r_1)}\pi(E' + C_{44})/2 + N(C_{11} - E')\frac{e^{\Delta} - 1}{e^{2r_1\Delta} - 1}(1 - e^{-r_1\Delta/l})\,, \tag{15}$$

for $N \neq 2$. When N=2, we have

$$\bar{K} = \frac{r_1}{(r_2 - r_1)}[\pi(E' + C_{44})/2 + (E^{'} - C_{44})] + 2(C_{11} - E')\frac{e^{\pi/4} - 1}{e^{2r_1\pi/4} - 1}(1 - e^{-r_1\pi/(4l)})\,, \tag{16}$$

for the lower edge of the bandgap, and

$$\bar{K} = \frac{r_1}{(r_2 - r_1)}[\pi(E' + C_{44})/2 - (E^{'} - C_{44})] + 2(C_{11} - E')\frac{e^{\pi/4} - 1}{e^{2r_1\pi/4} - 1}(1 - e^{-r_1\pi/(4l)})\,, \tag{17}$$

for the upper edge of the bandgap. The difference between the lower and upper edges is directly induced by the different roles of the coating in the vibration mode.

Substituting Eqs.(15)-(17) into Eqs. (6) and (7), we can evaluate the eigen frequencies at the bandgap edges, see Fig.4, where the thick-dashed and thick-solid lines represent the lower and upper edges of the bandgap, respectively. The agreement between the predicted results and the numerical ones is satisfied.

Moreover, the numerical results for the PCs in a triangular lattice are also plotted in Fig.4. The steel core, the coating and their filling ratio are exactly the same as those in the square lattice. The results confirm that the locally resonant gap is invariant with respect to the lattice symmetries [2]. In other words, the proposed model can evaluate the lowest bandgap for two-dimensional locally resonant PC with a comblike coating regardless of the lattice symmetry.

4. Conclusions

In summary, when a comblike coating is introduced to the ternary locally resonant PC, a complete bandgap at a lower frequency can be obtained, except for the

case of a comblike coating with two pieces. This is due to the fact that the thin layers of the 'plane-stress' state near the free surface can decrease the effective stiffness of the coating. The width of this low bandgap, which is a little smaller than that for a uniform coating, is nearly unchanged with its center frequency getting slightly low when the number of the pieces increases. An equivalent spring-mass model is proposed for a better understanding of the mechanism of the bandgap generation as well as evaluation of the corresponding bandgap edges. The research is relevant to the design of locally resonant PCs which have the potential applications in wave or noise control in the low (even audible) frequency range.

It is worthy to point out that this letter just provides a basic idea for the design of the locally resonant PCs with a comblike coating. Actually, a steel core coated with the comblike coating can be manufactured by wrapping the core with a thin layer of coating with many discrete pieces. The discrete piece can also be in other shape, such as parallelogram, trapezoid, etc. Distinguished features maybe expected with various comblike coatings.

Acknowledgements

The authors are grateful for the support from the National Natural Science Foundation of China (Grant No. 11272041), the National Basic Research Program of China (2010CB732104) and the Oslofjord Research Fond of Norway (RFFOFJOR-ES468298). The first author also acknowledges Rino Nilsen for fruitful discussion during his short visit at Fredrikstad.

Reference list

[1] M. S. Kushwaha, P. Halevi, L. Dobrzynski, and B. Djafari-Rouhani: Phys. Rev. Lett. **71** (1993) 2022.

[2] Z. Y. Liu, C. T. Chan, and P. Sheng: Phys. Rev. B **65** (2002) 165116.

[3] K. M. Ho, C. K. Cheng, Z. Yang, X. X. Zhang, and P. Sheng: Appl. Phys. Lett. **83** (2003) 5566.

[4] Z. Y. Liu, X. X. Zhang, Y. W. Mao, Y. Y. Zhu, Z. Y. Yang, C. T. Chan, and P. Sheng: Science **289** (2000) 1734.

[5] C. Goffaux, J. Sánchez-Dehesa, A. Levy Yeyati, Ph. Lambin, A. khelif, J. O. Vasseur, and B. Djadari-Rouhani: Phys. Rev. Lett. **88** (2002) 225502.

[6] M. Hirsekorn: Appl. Phys. Lett. **84** (2004) 3364.

[7] G. Wang, X. S. Wen, J. H. Wen, L. H. Shao, and Y. Z. Liu: Phys. Rev. Lett. **93** (2004) 154302.

[8] J. C. Hsu and T. T. Wu: Appl. Phys. Lett. 90 (2007) 201904.

[9] W. Xiao, G. W. Zeng, and Y. S. Cheng: Appl. Acoust. **69** (2008) 255.

[10] Z. Yang, J. Mei, M. Yang, N. H. Chan, and P. Sheng: Phys. Rev. Lett. **101** (2008) 204301.

[11] Y. Pennec, B. Djafari-Rouhani, H. Larabi, J. O. Vasseur, and A. C. Hladky-Hennion: Phys. Rev. B **78** (2008) 104105.

[12] T. T. Wu, Z. G. Huang, T. C. Tasi, and T. C. Wu: Appl. Phys. Lett. **93** (2008) 111902.

[13] M. Oudich, M. B. Assouar, and Z. L. Hou: Appl. Phys. Lett. **97** (2010) 193503.

[14] X. N. Liu, G. K. Hu, G. L. Huang, and C. T. Sun: Appl. Phys. Lett. **98** (2011) 061912.

[15] M. Oudich, Y. Li, M. B. Assouar, and Z. L. Hou: New J. Phys. **12** (2010) 083049.

[16] R. Zhu, G. L. Huang, H. H. Huang, and C. T. Sun: Phys. Lett. A **375** (2011) 2863.

[17] M. B. Assouar and M. Oudich: Appl. Phys. Lett. **100** (2012) 123506.

[18] G. Wang, L. H. Shao, Y. Z. Liu, and J. H. Wen: Chin. Phys. **15** (2006) 1843.

[19] Y. F. Wang, Y. S. Wang, and X. X. Su: J. Appl. Phys. **110** (2011) 113520.

Figure captions

Table I. Elastic parameters of the materials.

Table II. Band edges predicted by equivalent models for PC with a uniform coating under different geometrical parameters.

Fig.1 Configurations of the ternary PC with a comblike coating (a) and a uniform coating (b).

Fig.2 Band structures of the PC with (a) a comblike coating of 16 pieces and (b) a uniform coating in a square lattice, where r_1/a=0.27 and r_2/a=0.4.

Fig. 3 Vibration modes of displacements at the bandgap edges marked in Fig.2. Panels (a)-(d) correspond to points S1-S4, respectively.

Fig.4 Variations of bandgap edges with the number of the comblike coating for r_2/a=0.4 and r_1/a=0.27 (a) or r_1/a=0.33 (b). The scattered symbols represent the numerical results; and the solid and dashed lines represent the analytical results. The two dotted lines represent the results for PC with a uniform coating, the modulus of which is a half of rubber. □(△) — Lower edge for a square (triangular) lattice; ■ (▲) — Upper edge for a square (triangular) lattice. – – (- - - -) — Lower edge evaluated by using $E_r(\theta)(C_{11})$; ——(——) — Upper edge evaluated by using $E_r(\theta)(C_{11})$.

Fig.5 Vibration modes of displacements at the lower edge (a) and the upper edge (b) for PC with a coating of two pieces.

Fig.6 Explanation of the calculation method of parameters in the proposed model: (a) a sectorial piece, (b) its corresponding rectangular strip.

Fig.7 Strain energy versus the central angle for one sectorial piece and its corresponding rectangular strip under the same elongation. The solid and thick dashed lines represent the analytical results with n=1, 100, respectively.

Table I. Elastic parameters of the materials.

Materials	Core	Coating	Matrix
Mass density, ρ [kg/m^3]	8950	1020	1200
Young's modulus, E [Pa]	2.1×10^{11}	1×10^{5}	3.5×10^{7}
Poisson's ratio, ν	0.29	0.47	0.49

Table II. Band edges predicted by equivalent models for PC with a uniform coating under different geometrical parameters.

Geometry	r_1/a=0.27 and r_2/a=0.4		r_1/a=0.33 and r_2/a=0.4	
Band edges	Lower edge	Upper edge	Lower edge	Upper edge
FEM result	0.0714	0.130	0.0920	0.212
Present model	0.0705 (1.3%)	0.134 (3.1%)	0.0905 (1.6%)	0.209 (1.4%)
Model in Ref.[13]	0.0725 (1.5%)	0.135 (3.8%)	0.0907 (1.4%)	0.209 (1.4%)

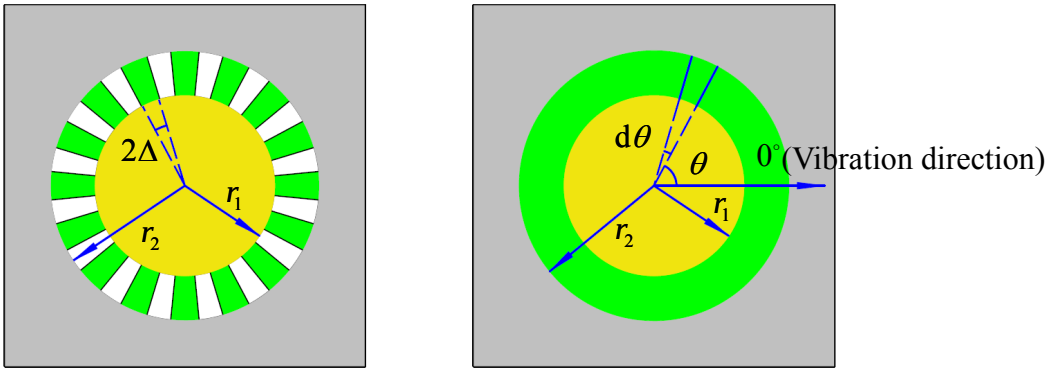

(a) (b)

Fig.1 Configurations of the ternary PC with a comblike coating (a) and a uniform coating (b).

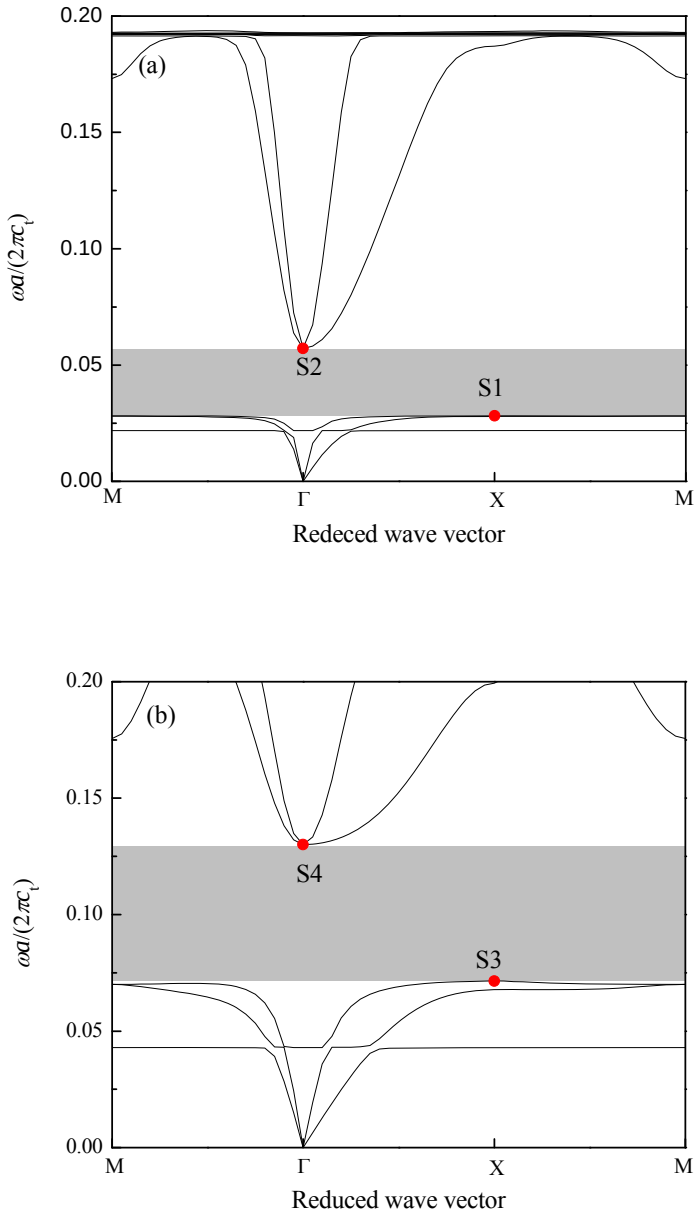

Fig.2 Band structures of the PC with (a) a comblike coating of 16 pieces and (b) a uniform coating in a square lattice, where r_1/a=0.27 and r_2/a=0.4.

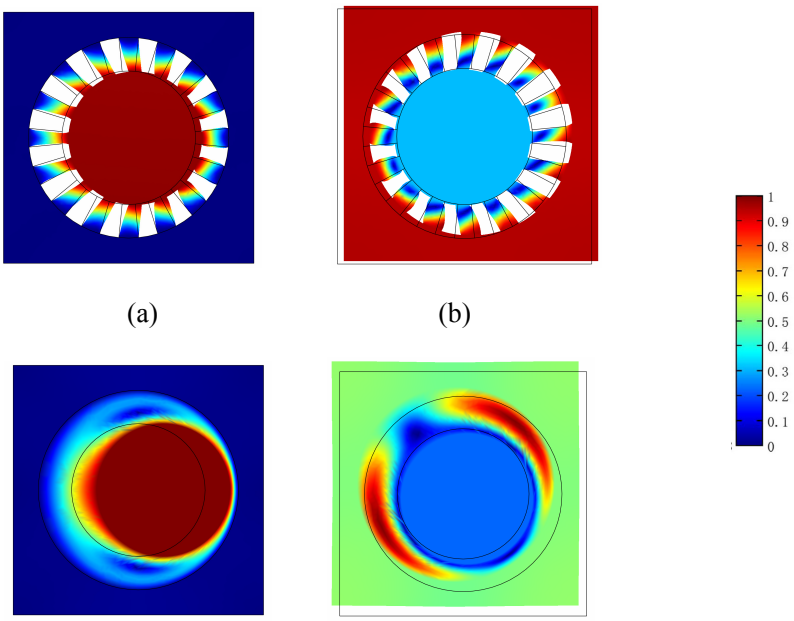

Fig. 3 Vibration modes of displacements at the bandgap edges marked in Fig.2. Panels (a)-(d) correspond to points S1-S4, respectively.

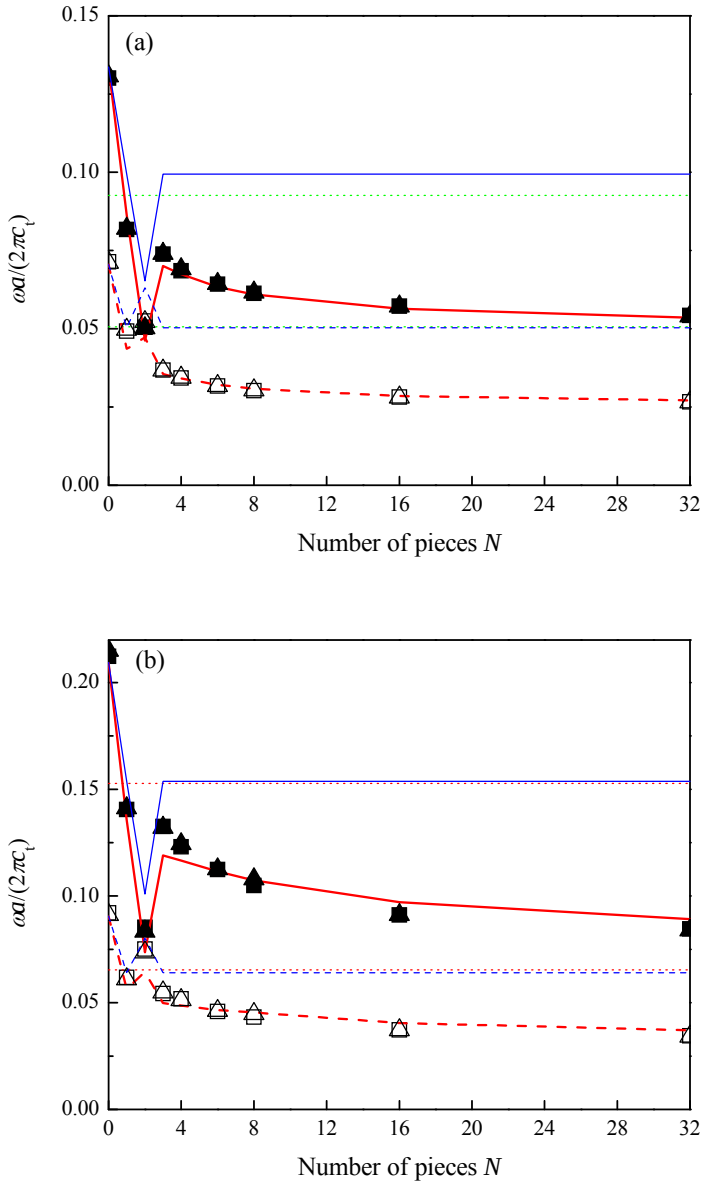

Fig.4 Variations of bandgap edges with the number of the comblike coating for r_2/a=0.4 and (a) r_1/a=0.27 or (b) r_1/a=0.33. The scattered symbols represent the numerical results; and the solid and dashed lines represent the analytical results. The two dotted lines represent the results for PC with a uniform coating, the modulus of which is a half of rubber. □(△) — Lower edge for a square (triangular) lattice; ■(▲) — Upper edge for a square (triangular) lattice. – – (- - - -) — Lower edge evaluated by using $E_r(\theta)(C_{11})$; ——(——) — Upper edge evaluated by using $E_r(\theta)(C_{11})$.

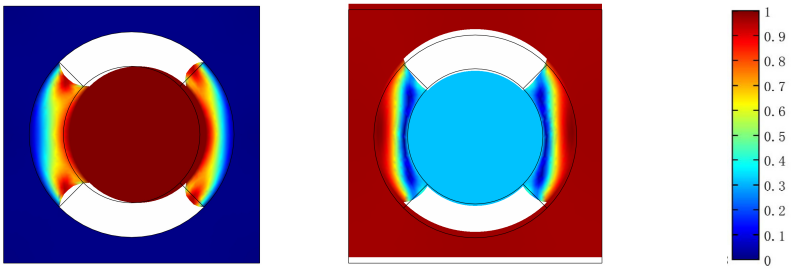

(a) (b)

Fig.5 Vibration modes of displacements at the lower edge (a) and the upper edge (b) for PC with a coating of two pieces.

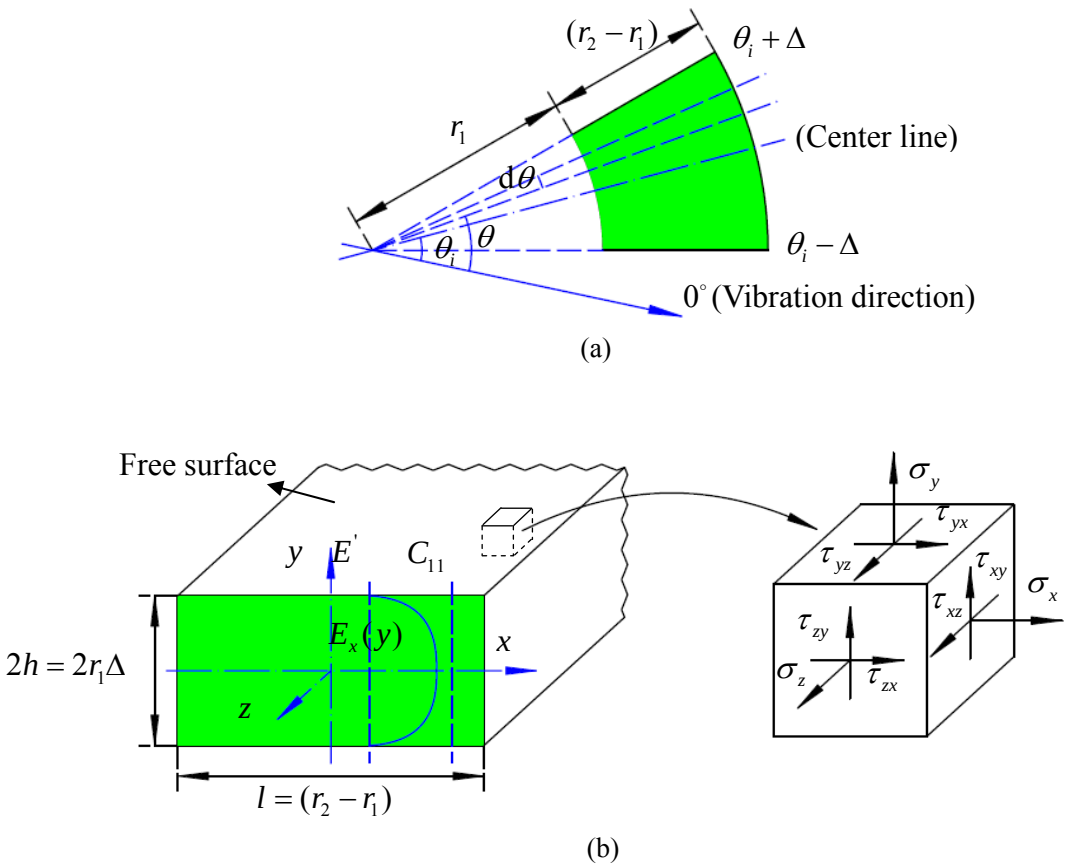

Fig.6 Explanation of the calculation method of parameters in the proposed model: (a) a sectorial piece, (b) its corresponding rectangular strip.

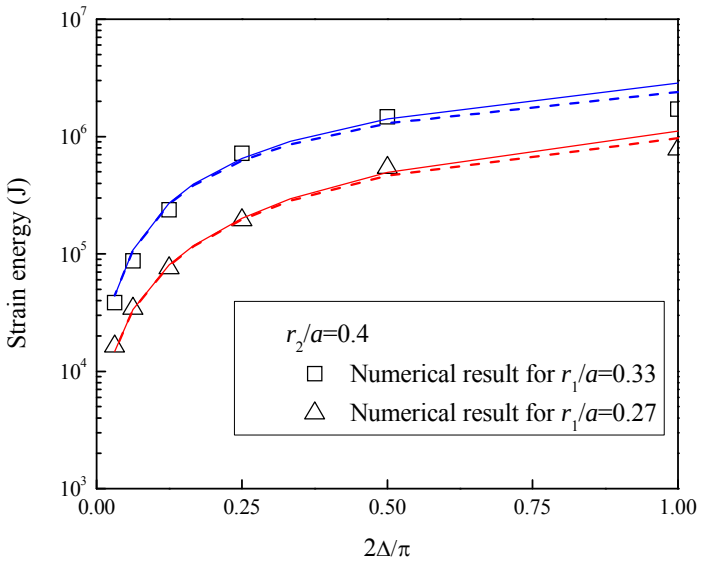

Fig.7 Strain energy versus the central angle for one sectorial piece and its corresponding rectangular strip under the same elongation. The solid and thick dashed lines represent the analytical results with n=1, 100, respectively.